

Polymer-Modified Halloysite Composite Nanotubes

Cuiping Li,¹ Jiguang Liu,¹ Xiaozhong Qu,¹ Baochun Guo,² Zhenzhong Yang¹

¹State Key Laboratory of Polymer Physics and Chemistry, Institute of Chemistry, Chinese Academy of Sciences, Beijing 100190, China

²Department of Polymer Materials and Engineering, South China University of Technology, Guangzhou 510640, China

Received 5 April 2008; accepted 10 June 2008

DOI 10.1002/app.28879

Published online 17 September 2008 in Wiley InterScience (www.interscience.wiley.com).

ABSTRACT: A natural clay halloysite, which is a kind of aluminosilicate with a predominantly nanosized hollow tubular structure, was modified by polymers achieving polymer-halloysite composite nanotubes. Polymer chains can grow from both interior and exterior surfaces of the halloysite nanotubes by atom transfer radical polymerization (ATRP). Eventually, the composite nanotubes were evolved to a core-shell coaxial structure after the interior cavity was fully covered by the polymer. After dissolution of the hal-

loysite template, polymeric nanotubes and nanowires were derived. The composition could be controlled from polymer to carbon after being treated at high temperature. The idea can be extended to a cast halloysite fabric resulting nonwoven composites, which had some interesting wettability. © 2008 Wiley Periodicals, Inc. *J Appl Polym Sci* 110: 3638–3646, 2008

Key words: halloysite; ATRP; composite nanotube; nonwoven fabric

INTRODUCTION

Nanocomposites have been widely investigated due to their unique properties and potential applications in optical, electronic, magnetic, and thermosensitive devices.^{1–4} Template-directed synthesis is commonly used to prepare such nanocomposites with well-controlled structures,⁵ and a diversity of templates from artificial to biological species are used. However, the approaches are relatively high in cost.^{6,7} Facile and more effective synthesis is urgently required for the fabrication of nanocomposites.

Recently, halloysite, as an economically available nanosized raw material, has gained growing interest to synthesize complex structures.^{8–11} Halloysite is mainly composed of aluminosilicate and has a predominantly hollow tubular structure. Template synthesis with metallic nanoparticles has resulted formation of nanowires and porous carbon materials.^{12–14} However, the synthesis is restricted within a narrow composition as specific interactions between grown materials and the template are required.¹² For example, the ineffective conjugation of the carbon precursors onto the template will lead to sheet alike carbon materials rather than carbon nanotubes.^{13,14}

It is important to modify the halloysite resulting polymer-halloysite nanocomposites with tubular structure well retained. Atom transfer radical polymerization (ATRP) has been extensively used to grow a diversity of polymer brushes onto either planar substrates or individual spheres surface.^{15,16} Herein, we reported on the extension of ATRP onto halloysite nanotubes toward their nanocomposites. Composition could be easily tuned by alteration of the monomer structure. Besides individual halloysite nanotubes, nonwoven composite fabrics could be synthesized by ATRP onto the corresponding cast halloysite fabric.

EXPERIMENTAL

Immobilization of ATRP initiator onto halloysite

The halloysite nanotube was immobilized with an ATRP initiator by a two-step method.¹⁷ After being treated with H₂O₂ at 80°C for 24 h, the halloysite was modified with 3-aminopropyltrimethoxysilane (APS) at 120°C in toluene for 12 h and then washed with ethanol. The silanized halloysite was further reacted with 2-bromoisobutyryl bromide in dry dichloromethane containing dry triethylamine at 25°C for 10 h. After the modified halloysite was repeatedly washed with acetone and ethanol, it was dried under vacuum prior to use.

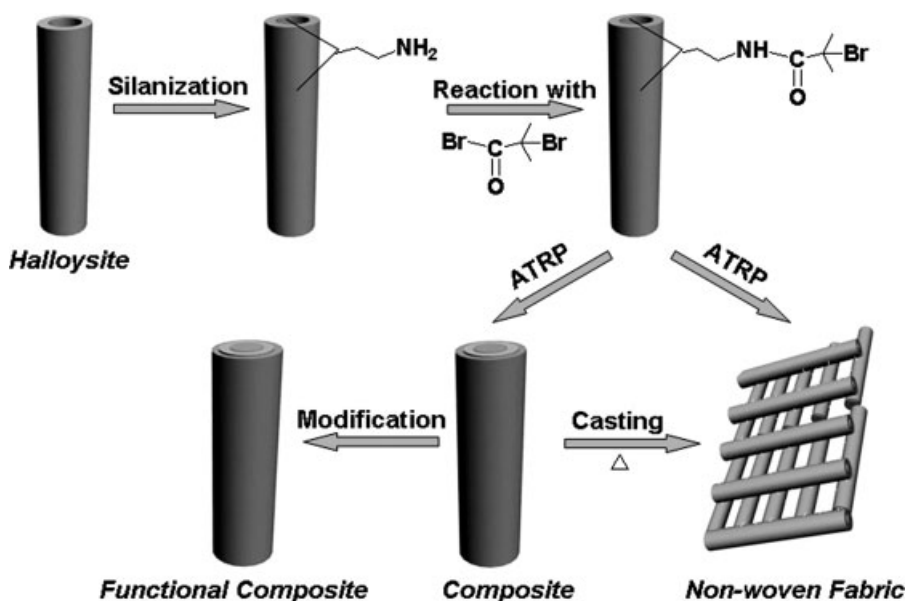
Synthesis of crosslinked PS/halloysite composites

In a typical experiment, 0.8 g (0.046 mmol initiator) of modified halloysite, 10 mL (87.4 mmol) of styrene

Correspondence to: Z. Yang (yangzz@iccas.ac.cn).

Contract grant sponsor: NSFC; contract grant numbers: 50325313, 90206025, 20128004, 50573083, 50603005.

Contract grant sponsor: Chinese Academy of Science, and the China Ministry of Science and Technology; contract grant numbers: KJJCX2-SW-H07, 2003CB615600.



Scheme 1 Illustrative synthesis of polymer-halloysite composite nanotubes and nonwoven fabric.

(St), 2.3 g (17.7 mmol) of divinylbenzene (DVB), 10.0 mL of toluene and 144 μL (0.7 mmol) of *N,N,N',N'',N'''*-pentamethyldiethylenetriamine (PMDETA) were mixed in a 50 mL dry flask equipped with a magnetic stirrer. After being purged with nitrogen, 0.03 g (0.2 mmol) of CuBr was added. Afterward, ATRP was carried out at 110°C for a varied time to control the grafting polymer content.

Synthesis of crosslinked PAN/halloysite composites

In a typical experiment, 0.8 g (0.046 mmol initiator) of modified halloysite, 10 mL (153.3 mmol) of acrylonitrile (AN), 4.0 g (30.7 mmol) of DVB, 10.0 g (113.6 mmol) of ethylene carbonate (EC) and 144 μL (0.7 mmol) of PMDETA were mixed in a 50 mL dry flask equipped with a magnetic stirrer. After being purged with nitrogen, 0.03 g (0.2 mmol) of CuBr and 0.001 g (0.02 mmol) of Cu were added. Afterward, ATRP was carried out at 55°C for a varied time to control the grafting polymer content.

Carbonization

After the crosslinked PAN/halloysite composite powder was preoxidated at 200°C for 10 h in an air atmosphere, it was further heated to a desired high temperature, for example 700°C at a rate 1.6°C min^{-1} , and held for 3 h in nitrogen. Free-carbon nanotubes and nanowires were formed by dissolution the halloysite by a HF/HCl mixture.

Characterization

Morphology and composition of the samples were performed with a Hitachi S-4300 scanning electron microscope (SEM) equipped with an energy-dispersive X-ray (EDX) analyzer operated at an accelerating voltage of 15 kV. The samples were ground into powders and dispersed in ethanol under ultrasonication. The dispersions were dropped onto carbon coated copper grids for transmission electron microscopy (TEM) characterization (JEOL 100CX operating at 100 kV). Elemental analysis was carried out using a Flash EA-1112 apparatus. BET-specific surface area was characterized by nitrogen adsorption/desorption on a Micromeritics ASAP 2020M surface area and porosity analyzer. The dried samples were pressed into pellets with potassium bromide (KBr) and characterized by a BRUKER EQUINOX 55 FTIR spectrophotometer. Polymer content of the composite materials was measured by Perkin-Elmer Pyris 1 TGA under nitrogen. The crystalline phases of the materials were characterized by wide-angle X-ray powder scattering (Rigaku D/max-2500). The molecular weight and distribution of the polymers were determined using a gel permeation chromatography (GPC) equipped with Waters Microstyrigel columns (HT2, HT3, and HT4) and a Waters 515 High Performance Liquid Chromatograph (HPLC), with a 2410 refractive index detector. Measurements were conducted in tetrahydrofuran (30°C) at a flow rate of 1 mL/min. Polystyrene standards were used to generate the calibration curve. ^1H NMR spectra were recorded on a Bruker AV 400-MHz spectrometer with CDCl_3 as the solvent and tetramethylsilane as an internal standard. Contact angle of the nonwoven

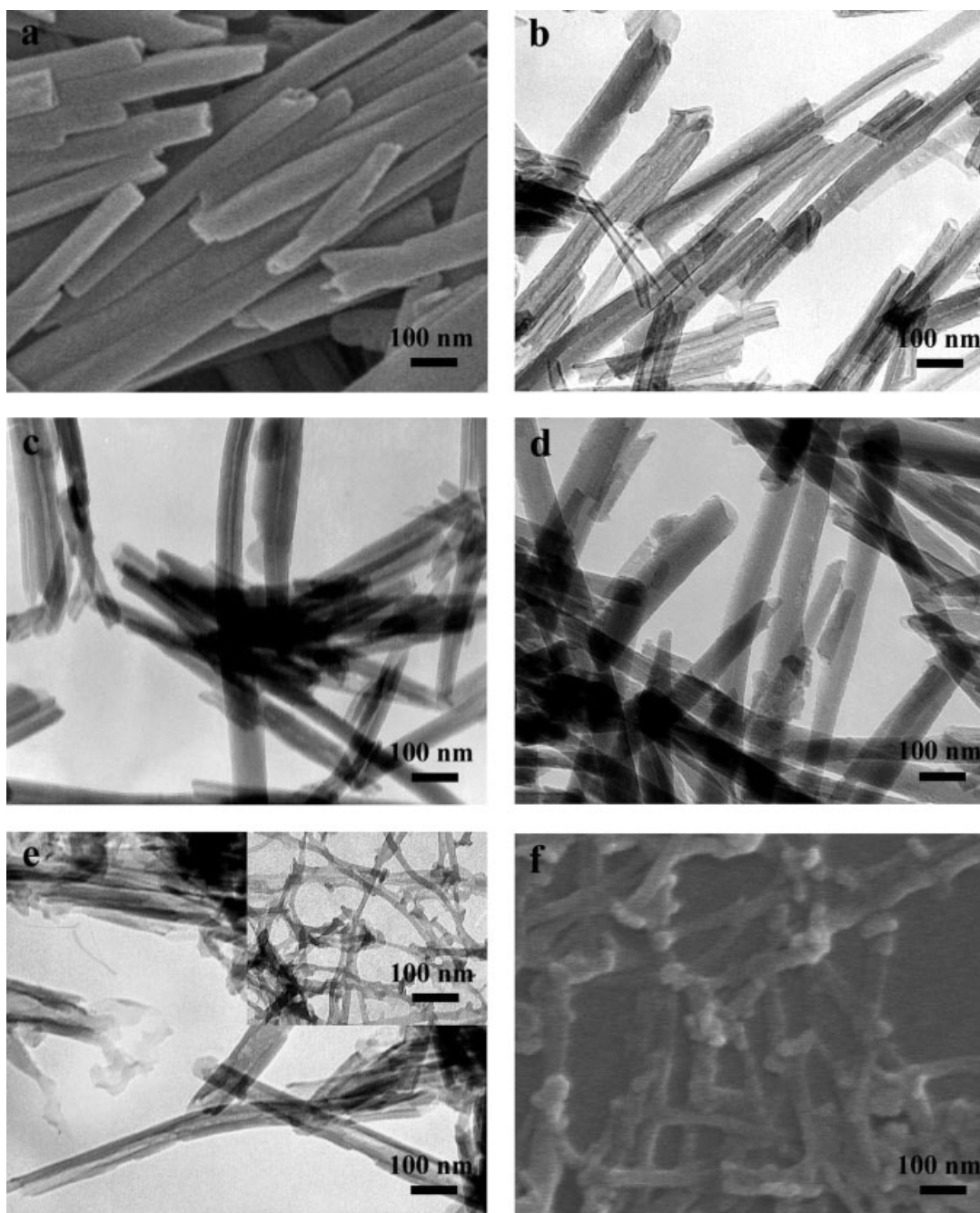


Figure 1 SEM and TEM images of some representative crosslinked PAN/halloysite composite nanotubes: (a,b) the halloysite nanotubes; (c,d) the crosslinked PAN/halloysite composite nanotubes; (e,f) the crosslinked PAN nanotubes and nanowires after the halloysite was dissolved by HF/HCl.

fabrics was measured with an optical contact angle meter at ambient temperature. The water droplets are 1–2 mm in diameter.

RESULTS AND DISCUSSION

The halloysite nanotube (purchased from Imerys Tableware Asia Limited) was selected as a model.¹⁸ Both interior and exterior wall surfaces can be modified with silanes. As illustrated in Scheme 1, ATRP

is first carried out synchronously onto the surfaces to gain polymer-halloysite composite nanotubes. To strengthen the polymeric brushes, additional crosslinkers should be added. Then polymer-halloysite composite nonwoven fabrics can be achieved by casting the dispersion of the polymer coated halloysite nanotubes or ATRP onto the corresponding cast halloysite fabric. Finally, the halloysite template is etched with HF/HCl mixture to generate corresponding polymer materials. In our study, two

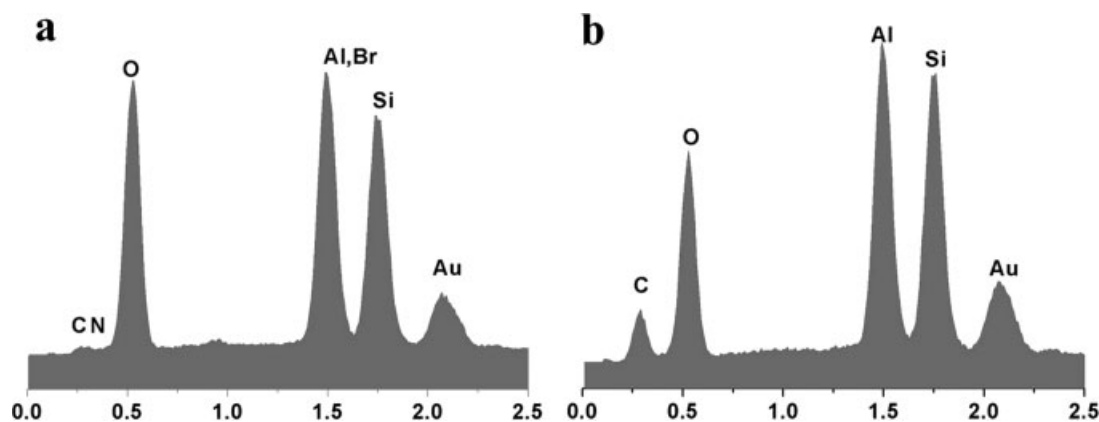


Figure 2 EDX spectra of (a) the initiator-modified halloysite nanotube (ha-Br) and (b) the crosslinked PS/halloysite composite nanotube.

representative polymers: polystyrene (PS) and polyacrylonitrile (PAN) were chosen, as they could be easily modified to derive functional groups facilitating the formation of composites with various compositions.¹⁹

The halloysite is predominately tubular with a length 1–2 μm and an inner diameter 20–30 nm. The shell thickness is 10–15 nm [Fig. 1(a,b)]. After being modified with APS and 2-bromoisobutyrate, C, N, and Br elements were detected by EDX [Fig. 2(a)]. FTIR spectra of the modified halloysite (ha-Br) (Trace b, Fig. 3) showed sharp vibration bands at 3000–2870 and 1540 cm^{-1} diagnostic for the saturated hydrocarbon and Amide II ($-\text{CONH}-$) which were not present in the IR spectra of the starting halloysite (Trace a, Fig. 3). And further elemental analysis indicated that the modified halloysite contained 0.46% of bromine on average, whereas the starting halloysite contained <0.03%. This difference translated into an average amount of 0.058 mmol of initiator was immobilized in 1 g of modified halloysite.

The surface-modified halloysite (ha-Br) were then used as macroinitiators for the ATRP of styrene at 110°C. The experimental conditions were the same as that of synthesis of crosslinked PS/halloysite composites in the absence of crosslinker DVB. After being polymerized for 3 h, the inner diameter decreased to several nanometers [Fig. 4(b)]. With prolonging polymerization time and increasing feed of the monomer, the thickness of polymer brushes also increased (Fig. 4). Eventually, the interior cavity was completely filled with crowded polymer brush [Fig. 4(c)], for example after being polymerized for 4.5 h. These results indicated the thickness of both outer and inner layer of the polymer can be controlled by tuning the reaction time.

To further confirm that the grafting polymerization is controlled, the polystyrene graft chains were cut from the backbone by dissolution of halloysite

with HF/HCl. The molecular weight of the grafted polymer, as determined with GPC, increased with the polymerization time (Fig. 5). It is also seen in Figure 5 that the diagrams contain two peaks with relatively close elution time for all specimen sampled at 1.5–6 h, indicating two dynamics with slightly different rate occurred throughout the polymerization. This was attributed to the difference of the polymerization position on the halloysite tubes, i.e., the inner and outer surface, as both of the peaks shift to shorter elution volume with the increase of

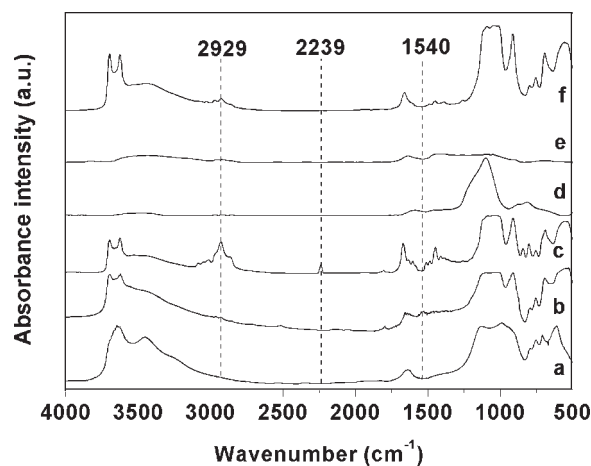


Figure 3 FTIR spectra of some representative polymer/halloysite nanocomposites: (a) the halloysite; (b) the initiator modified halloysite (ha-Br); (c) the crosslinked PAN/halloysite composite; (d) the C/halloysite composite after the crosslinked PAN/halloysite composite was carbonized at 700°C; (e) C after the halloysite was removed from the C/halloysite composite; (f) the crosslinked PS/halloysite composite. The characteristic band at 2239 cm^{-1} was assigned to nitrile group ($-\text{CN}$), which disappeared after carbonization. The characteristic band at 1540 cm^{-1} was assigned to amide II ($-\text{CONH}-$) which appeared after immobilization of ATRP initiator. The characteristic bands between 2950 and 2850 cm^{-1} were assigned to the hydrocarbonated $-(\text{CH}_2-\text{CH})_n-$ backbone.

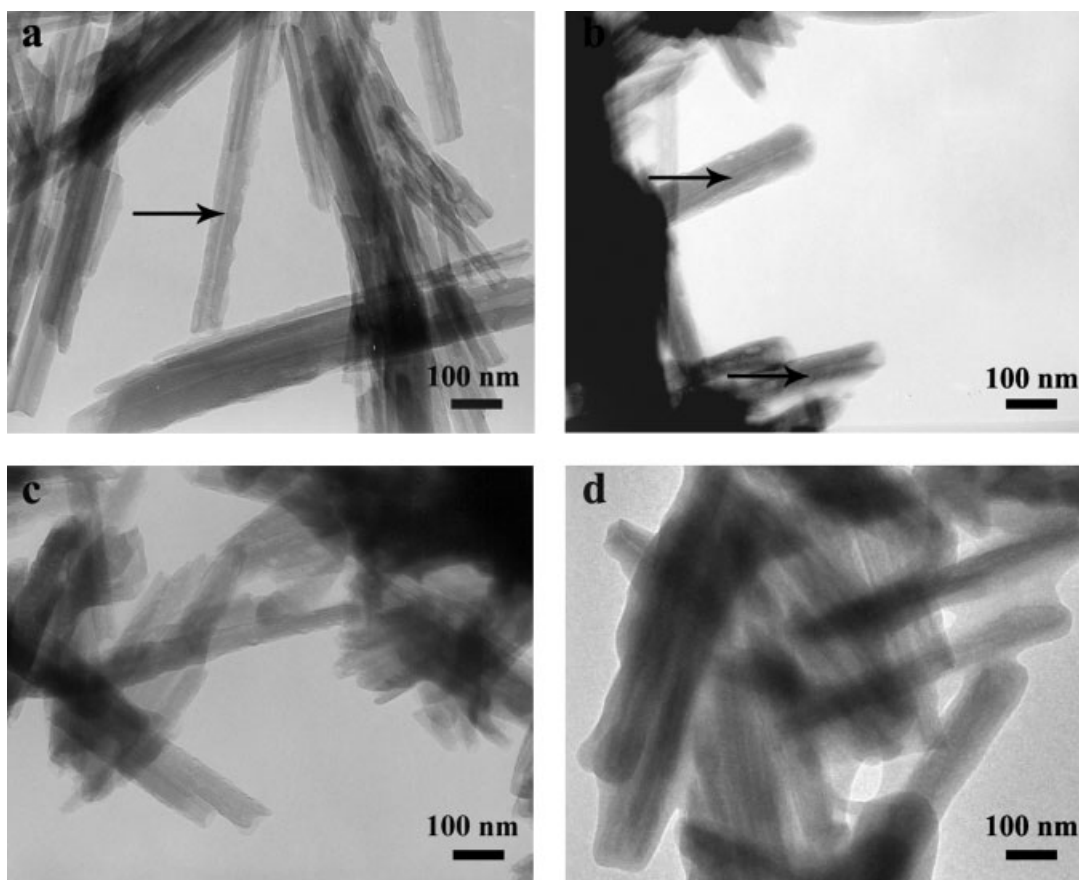


Figure 4 TEM images of PS/halloysite composite nanotubes obtained at different polymerization time via ATRP process at 110°C. The polymerization time were 1.5 h, 3 h, 4.5 h and 6 h for a, b, c, and d, respectively. Experimental conditions: [St] : [ha-Br] : [CuBr] : [PMDETA] = 437 : 0.23 : 1 : 3.46, in toluene at 110°C.

reaction time, an indication of chain growth, inferring that it was not caused by a thermo polymerization. Instead, at longer reaction times, e.g., 4.5 h and 6 h, the ratio of the lower molecular weight portion

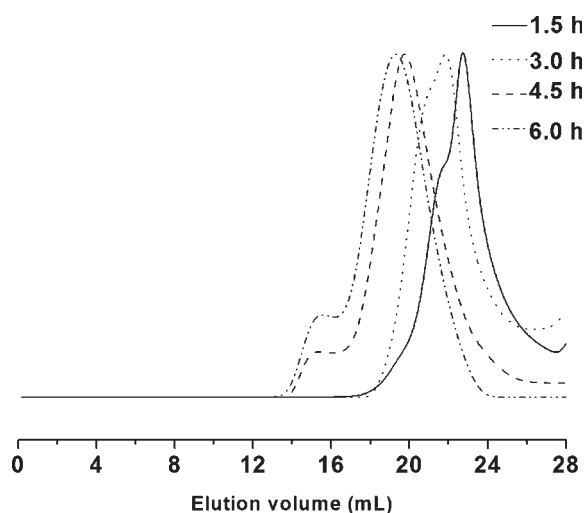


Figure 5 GPC traces of polystyrene graft chains cleaved from the halloysite by dissolution with HF/HCl. Experimental conditions see Figure 4.

to the higher molecular weight portion became larger as demonstrated from the integrals of the peaks in Figure 5, which was explained by the prohibited growth of PS within the interior cavity due to the limited space. The disappearance of the hollow cavity [Fig. 4(d)] supported the presumption. Figure 6 showed the ^1H NMR spectrum of the cleaved PS graft ($M_{n,\text{GPC}} = 65,000$; $t = 3$ h). The signals *a* at 1.01–2.28 ppm were ascribed to the methine

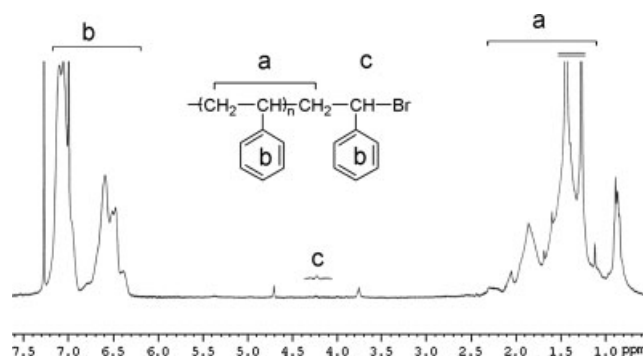


Figure 6 ^1H NMR spectrum of the polystyrene graft chains cleaved from the halloysite ($M_{n,\text{GPC}} = 65,000$; $t = 3$ h).

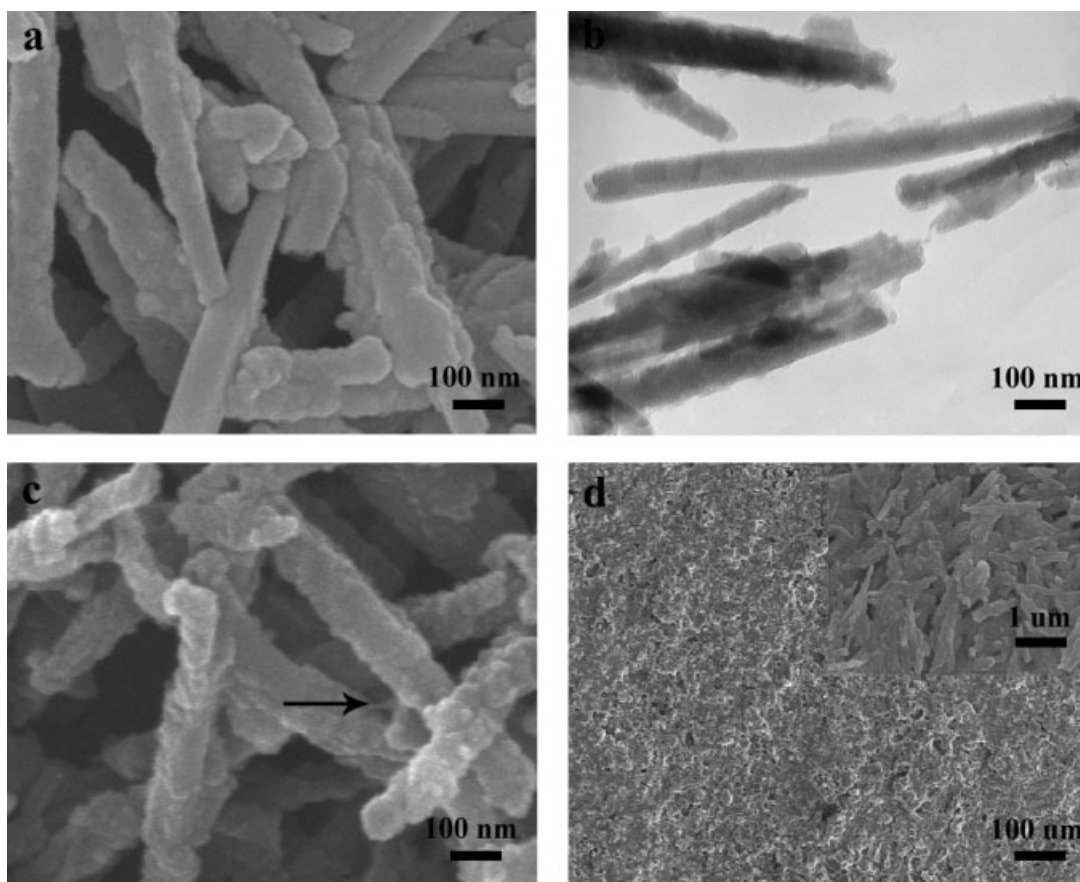


Figure 7 SEM and TEM images of some representative crosslinked PS/halloysite composite: (a,b) the crosslinked PS/halloysite composite nanotubes; (c) the crosslinked PS nanotubes and nanowires after the halloysite was dissolved; and (d) the crosslinked PS/halloysite nonwoven fabric.

proton and methylene protons of styrene monomer. The signals *b* at 6.32–7.24 ppm were attributed to the five aromatic protons of styrene unit. The signals of the end-standing methine proton next to the bromine were detected at 4.20–4.40 ppm as *c*. Taken together, the experimental data were consistent with a controlled radical polymerization of styrene from the surface of the halloysite to yield PS/halloysite composite.

The corresponding nanotube consisting of linear PS inclined to collapse after removal the template. To gain the intact polymer nanotube after removal of the template, additional crosslinkers, for example DVB, were added. Using the same procedure, crosslinked PS/halloysite composite material was accordingly synthesized [Fig. 7(a,b)]. FTIR spectra of the product showed vibration bands corresponding to both polystyrene and silica (Trace f, Fig. 3). The interior cavity was gradually crowded with polymer brushes as indicated by the decreased BET specific surface area with ATRP time [$48 \text{ m}^2 \text{ g}^{-1}$ (0 h), $42 \text{ m}^2 \text{ g}^{-1}$ (1.5 h), and $28 \text{ m}^2 \text{ g}^{-1}$ (3 h)]. TGA result showed an increased weight loss from 18.4 wt % of the original halloysite to 24 wt % (1.5 h) and eventually 34.6

wt % (3 h) (Fig. 8). This result was also consistent with the increase of C element measured by EDX spectra from 10.4 at % of the initiator modified halloysite [Fig. 2(a)] to 22.1 at % (1.5 h) and 37.4 at % (3 h) [Fig. 2(b)], respectively. Element analysis

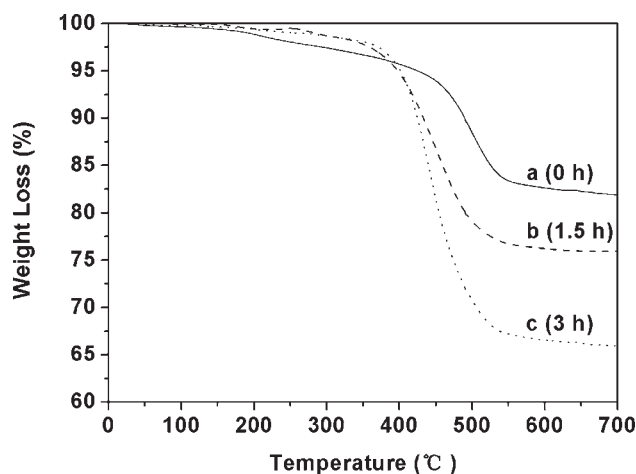


Figure 8 TGA curve of crosslinked PS/halloysite composite prepared at different ATRP time.

TABLE I
Composition of Polymer-Grafted Halloysite

| System | Reaction time (h) | Monomer unit in copolymer (mol %) ^a | Polymer in the modified halloysite (wt %) |
|---|-------------------|--|---|
| Crosslinked PAN/halloysite composite ^b | 2 | 50.6 ^a | 11.6 ^a |
| | 4 | 61.8 ^a | 21.5 ^a |
| | 6 | 68.2 ^a | 28.1 ^a |
| | 12 | 60.5 ^a | 37.1 ^a |
| Crosslinked PS/halloysite composite ^c | 1.5 | – | 14.5 ^d |
| | 3 | – | 26.1 ^d |

^{a,d} Calculated from the data of EDX and elemental analysis, respectively.

^b Reaction conditions: [AN] : [DVB] : [ha-Br] : [CuBr] : [Cu] : [PMDETA] = 760 : 152 : 0.23 : 1 : 0.1 : 3.46, [AN] = 15.2 M, in EC at 55 °C.

^c [St] : [DVB] : [ha-Br] : [CuBr] : [PMDETA] = 437 : 87 : 0.23 : 1 : 3.46, [St] = 4.37 M, in toluene at 110 °C.

also showed the content of PS increased with time (Table I). The wall thickness of the composite materials can be tuned by reaction time and monomer feed. The interior cavity was completely filled with PS brushes after prolonging polymerization time, for example 3 h. After removal of halloysite by dissolution, the corresponding nanotubes and nanowires were also achieved [Fig. 7(c)].

Besides individual halloysite, nonwoven fabrics could be easily prepared by casting the dispersions of the individual composite nanotubes. As the individual composite nanotubes contain residual vinyl-groups from DVB, the membrane was crosslinked at an elevated temperature. The porous membrane

could not be destroyed in the presence of solvents [Fig. 7(d)]. The nonwoven fabric became hydrophobic with a water contact angle $150.0 \pm 1.6^\circ$ [Fig. 9(a)]. The water droplets can be tightly entrapped by the fabric when the substrate was tilted vertically [Fig. 9(b)], even turned upside down [Fig. 9(c)]. This can be explained by the nanoscale structure and the high adhesion between water and PS layer.²⁰ The nonwoven fabric of nanofibers or nanotubes will have potential application in filtration, cell dissepiments, medical prostheses, tissue template, and wound dressing.²¹

The method is extended to other polymers, for example PAN. Crosslinked PAN/halloysite composite material was accordingly synthesized [Fig. 1(c,d)]. FTIR spectra of the product showed the vibration bands corresponding to both PAN and silica (Trace c, Fig. 3). After being polymerized for 4 h, the inner diameter decreased to several nanometers [Fig. 1(c)]. With prolonging polymerization time and increasing feed of the monomer, the

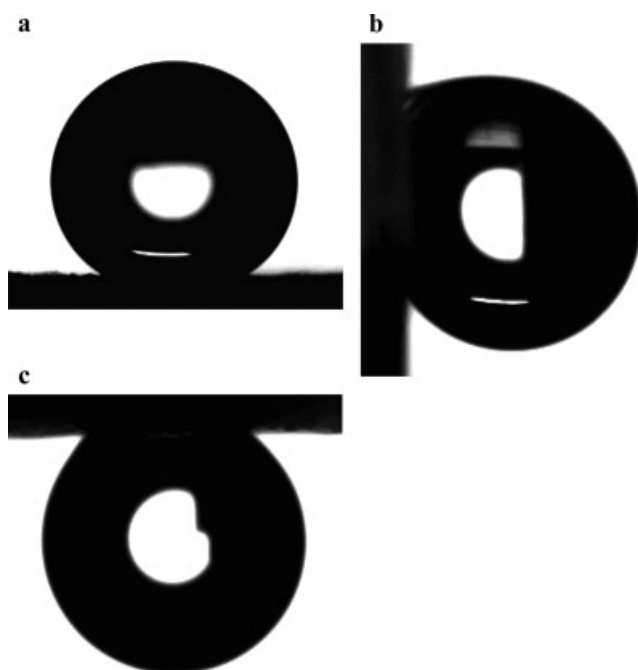


Figure 9 Profile of a water droplet on the as-prepared crosslinked PS/halloysite composite nonwoven fabric at different tilt angles. (a) 0°; (b) 90°, and (c) 180°.

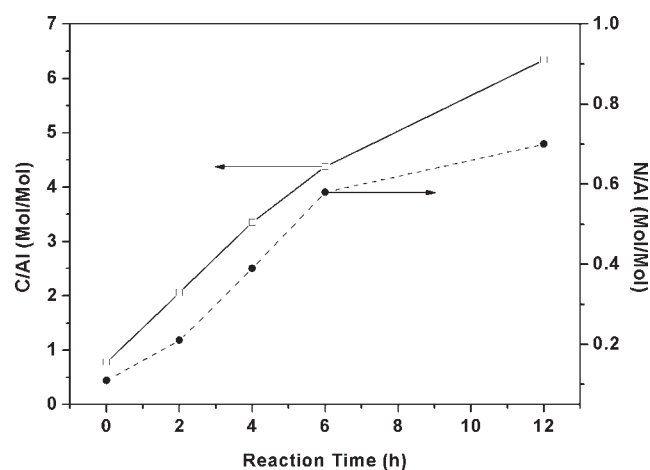


Figure 10 The crosslinked PAN content with polymerization time.

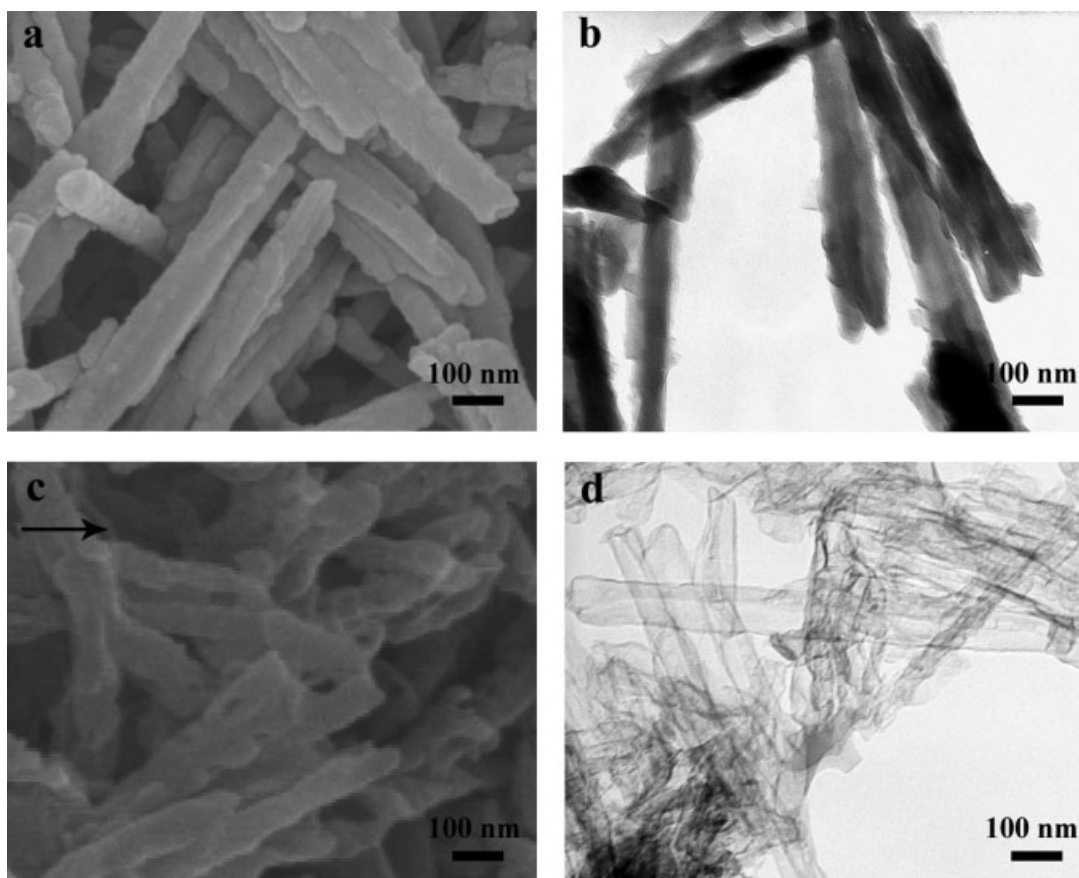


Figure 11 SEM and TEM images of some representative carbon samples: (a,b) the C/halloysite composite nanotubes; (c,d) C composites after removal of halloysite from the C/halloysite composite.

thickness of polymer brushes also increased. Eventually, the interior cavity was completely filled with crowded polymer brush [Fig. 1(d)], for example after being polymerized for 6 h. This was consistent with a PAN content indicated by the element N increased with polymerization time. Below polymerization time 6 h, the elements C and N increased quickly (Fig. 10). Above 6 h, the elements C and N increased slowly. This can be explained by the prohibited growth of PAN within the interior cavity as there has been crowded. This is agreed with the disappearance of the hollow cavity. Table I shows the composition of this polymer grafted halloysite. After being treated with HF/HCl mixture to dissolve the halloysite, both polymer nanotubes and smaller nanowires coexisted [Fig. 1(e)]. Expanded blobs were observed at the ends [Fig. 1(f)]. This is explained by a slippage of the nanowires in the interior cavity from the outer sheath.

PAN can be easily converted into carbon materials at high temperature.^{22,23} By the similar process, cross-linked PAN/halloysite composite nanotube was converted into a C/halloysite composite at 700°C [Fig. 11(a,b)]. The formation of carbon has been verified by FTIR spectra (Traces d, e, Fig. 3). Two bands at 1580

cm^{-1} and 1360 cm^{-1} corresponding to G and D bands were found (Fig. 12). X-ray diffraction (XRD) pattern showed two broad diffraction peaks at ~ 23 and 43° (Fig. 13). All the results revealed the obtained carbon was amorphous.²⁴ A slightly higher carbonization temperature, for example 900°C remained resultant

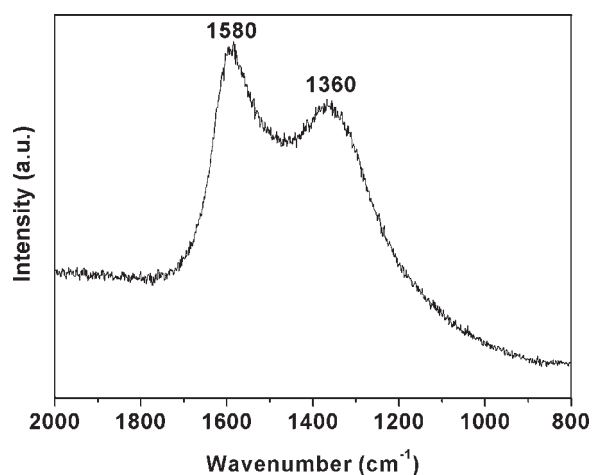


Figure 12 Raman spectrum of the C composite.

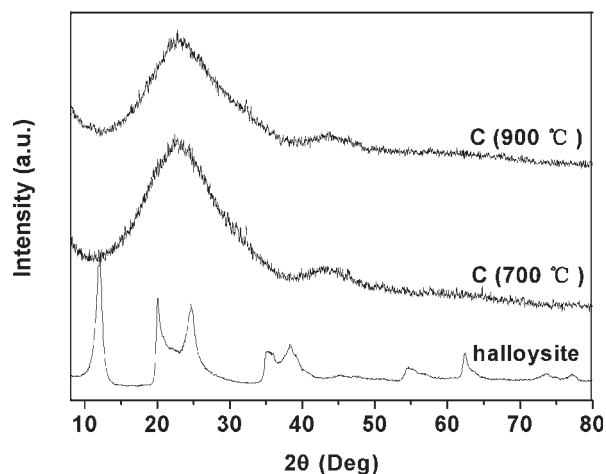


Figure 13 XRD results of the C material and halloysite.

amorphous carbon. After the halloysite template was removed, carbon nanotubes were prepared with an average cavity diameter of ~ 60 nm [Fig. 11(c,d)]. Such nanotube structure was better preserved than other materials by infiltration of carbon precursors.^{13,14,25}

CONCLUSIONS

A facile method had been developed for the synthesis of one-dimensional composites by grafting polymers onto halloysite nanotubes via ATRP. The interior cavity size can be continuously tuned by polymerization time and monomer feeding amount. After dissolution of halloysite, the corresponding polymeric and their derivative nanotubes and nanowires were derived. Furthermore, a nonwoven porous fabric was prepared by a direct cast of the composite dispersion followed by a sequent thermal crosslinking. The nonwoven fabric was highly hydrophobic and could tightly entrap water droplets.

References

1. Iijima, S. *Nature* 1991, 354, 56.
2. Patzke, G. R.; Krumeich, F.; Nesper, R. *Angew Chem Int Ed* 2002, 41, 2446.
3. Rao, C. N. R.; Nath, M. *Dalton Trans* 2003, 1, 1.
4. Sun, T. L.; Liu, H.; Song, W. L.; Wang, X.; Jiang, L.; Li, L.; Zhu, D. B. *Angew Chem Int Ed* 2004, 43, 4663.
5. Zhao, D.; Feng, J.; Huo, Q.; Melosh, N.; Fredrickson, G. H.; Chmelka, B. F.; Stucky, G. D. *Science* 1998, 279, 548.
6. Han, S. K.; Lee, T. S.; Oh, M.; Hyeon, T. *Carbon* 2003, 41, 1049.
7. Böhme, K.; Einicke, W. D.; Klepel, O. *Carbon* 2005, 43, 1918.
8. Joussein, E.; Petit, S.; Churchman, J.; Theng, B.; Righi, D.; Delvaux, B. *Clay Minerals* 2005, 40, 383.
9. Antill, S. J. *Aust J Chem* 2003, 56, 723.
10. Shchukin, D. G.; Sukhorukov, G. B.; Price, R. R.; Lvov, Y. M. *Small* 2005, 1, 510.
11. Lu, Z.; Eadula, S.; Zheng, Z.; Xu, K.; Grozdits, G.; Lvov, Y. *Colloids Surf A* 2007, 292, 56.
12. Fu, Y.; Zhang, L. *J Solid State Chem* 2005, 178, 3595.
13. Wang, A.; Kang, F.; Huang, Z.; Guo, Z. *Clays Clay Miner* 2006, 54, 485.
14. Wang, A.; Kang, F.; Huang, Z.; Guo, Z.; Chuan, X. *Micropor Mesopor Mater* 2008, 108, 318.
15. Kamigaito, M.; Ando, T.; Sawamoto, M. *Chem Rev* 2001, 101, 3689.
16. Matyjaszewski, K.; Xia, J. *Chem Rev* 2001, 101, 2921.
17. Steinle, E. D.; Mitchell, D. T.; Wirtz, M.; Lee, S. B.; Young, V. Y.; Martin, C. R. *Anal Chem* 2002, 74, 2416.
18. Technical Report of Imerys Tableware Asia Limited. Available at: <http://www.imerys-tableware.com/halloy.html>.
19. Yang, Z.; Niu, Z.; Lu, Y.; Hu, Z.; Han, C. C. *Angew Chem Int Ed* 2003, 42, 1943.
20. Jin, M.; Feng, X.; Feng, L.; Sun, T.; Zhai, J.; Li, T.; Jiang, L. *Adv Mater* 2005, 17, 1977.
21. Huang, Z.; Zhang, Y.; Kotaki, M.; Ramakrishna, S. *Compos Sci Technol* 2003, 63, 2223.
22. Lu, A.; Kiefer, A.; Schmidt, W.; Schuth, F. *Chem Mater* 2004, 16, 100.
23. Bu, H.; Rong, J.; Yang, Z. *Macromol Rapid Commun* 2002, 23, 460.
24. Setnescu, R.; Jipa, S.; Setnescu, T.; Kappel, W.; Kobayashi, S.; Osawa, Z. *Carbon* 1999, 37, 1.
25. Liu, G.; Kang, F.; Li, B.; Huang, Z.; Chuan, X. *J Phys Chem Solids* 2006, 67, 1186.